RSC Advances

PAPER

View Article Online
View Journal | View Issue



Cite this: *RSC Adv.*, 2017, **7**, 18650

# Two pairs of Zn(II) coordination polymer enantiomers based on chiral aromatic polycarboxylate ligands: synthesis, crystal structures and properties†

Ji-Han Huang,[ab] Guang-Feng Hou,[b] Dong-Sheng Ma,[a] Ying-Hui Yu,*[a] Wen-Hong Jiang,[a] Qi Huang[a] and Jin-Sheng Gao*[ab]

Received 9th January 2017
Accepted 23rd March 2017

DOI: 10.1039/c7ra00337d

rsc.li/rsc-advances

Two pairs of Zn-based chiral coordination polymers (**CCPs**), namely, [Zn((*R*)-cbca)·$H_2O$], [Zn((*S*)-cbca)]·$H_2O$], [Zn((*R*)-cna)·$2H_2O$] and [Zn((*S*)-cna)·$2H_2O$] {$H_2$cbca = (*R*) or (*S*)-4′-(1-carboxyethoxy)-[1,1′-biphenyl]-4-carboxylic acid, $H_2$cna = (*R*) or (*S*)-6-(1-carboxyethoxy)-2-naphthoic acid} were synthesized under hydrothermal conditions. Their structures were determined by single-crystal X-ray diffraction analysis and further characterized by elemental analysis, infrared spectroscopy, powder X-ray diffraction, circular dichroism (CD) spectroscopy. **CCPs 1–4** crystallized in chiral space groups and the CD spectra demonstrate obvious positive or negative Cotton effects. Second-harmonic generation (SHG) measurements show that **CCPs 1–4** are SHG active and the SHG efficiencies are 0.6, 0.6, 0.5 and 0.5 times as much as that of urea, respectively. **CCPs 1–4** exhibit relatively high luminescence properties originating from ligand centered emission.

## Introduction

As an emerging class of molecule-based hybrid materials, coordination polymers (CPs) have presented a promising prospect for various applications, including catalysis, recognition of small molecules, separation, magnetism, and luminescence.[1] In particular, chiral coordination polymers (**CCPs**) appear to be excellent candidates in the fields of enantiomorph separation, drug delivery, asymmetric catalysis, luminescence and sensors for their tunable structures, active sites with different strengths and their uniform size of channels or cavities present in the frameworks.[2] It is believed that the properties of **CCPs** have a direct relationship with their structures. However, the rational design and construction of coordination polymers (CPs) is still a continuing challenge, representing an ambitious goal for chemists.

At present, adopting homochiral ligands as building blocks has been proved to be the most reliable and effective way in the construction of **CCPs**.[3] Accordingly, how to design and obtain enantiopure ligands is of particular importance. Among different types of organic linkers, carboxylate donor ligands with strong coordination ability could satisfy various geometric requirements of metal centers by their diverse coordinating modes, which are capable of generating intriguing frameworks with high dimensions and interesting topologies.[4] The design and synthesis of new polycarboxylate based ligands have been one of ongoing research in our laboratory.[5] As an inexpensive, nontoxic and readily available material, lactic acid could be used as an ideal chiral source to incorporate chiral functional group to an organic ligand.[6]

Taking these into account, we presented here two pairs of chiral dicarboxylic acid enantiomers, namely, (*R*) or (*S*)-4′-(1-carboxyethoxy)-[1,1′-biphenyl]-4-carboxylic acid and (*R*) or (*S*)-6-(1-carboxyethoxy)-2-naphthoic acid ((*R*)-$H_2$cbca, (*S*)-$H_2$cbca, (*R*)-$H_2$cna and (*S*)-$H_2$cna) (Scheme 1), which are synthesized from homochiral lactic acid reacting with methyl 4′-hydroxy-[1,1′-biphenyl]-4-carboxylate and methyl 6-hydroxy-2-naphthoate, respectively. The design of the two pairs of new chiral ligands is also based on the following consideration: two structural units of naphthalene and diphenyl groups are introduced into the two pairs of ligands for comparison, as such structural diversity endows the two ligands different lengths and rigidness. It might be interesting and meaningful to investigate whether such slight difference in the ligands could have certain impact on the structures and properties of the eventual **CCPs** or not. We have now successfully prepared two pairs of Zn-based **CCPs**, namely, [Zn((*R*)-cbca)]·$H_2O$], [Zn((*S*)-cbca)]·$H_2O$], [Zn((*R*)-cna)·$2H_2O$] and [Zn((*S*)-cna)·$2H_2O$] *via* the

[a]*School of Chemistry and Materials Science, Heilongjiang University, Harbin 150080, China. E-mail: yuyinghui@hlju.edu.cn; gaojinsheng@hlju.edu.cn; Fax: +86 451 86609151; Tel: +86 451 86609001*

[b]*Engineering Research Center of Pesticide of Heilongjiang University, Heilongjiang University, Harbin 150080, China*

† Electronic supplementary information (ESI) available: Tables S1 and S2 and Fig. S1–S16. CCDC 1526162–1526165 for **1–4**. For ESI and crystallographic data in CIF or other electronic format see DOI: 10.1039/c7ra00337d

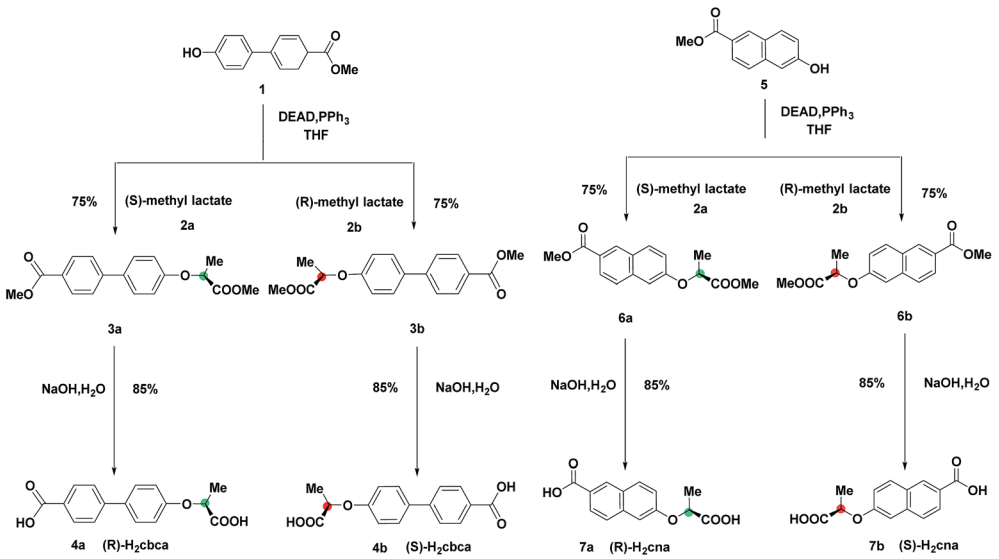


Scheme 1 Synthetic routes of the ligands (*R*)-$H_2$cbca, (*S*)-$H_2$cbca, (*R*)-$H_2$cna and (*S*)-$H_2$cna.

hydrothermal method. Herein, we report their synthesis, crystal structures, thermal stabilities, CD spectra, luminescence and second-order nonlinear optical properties.

## Experimental

### Materials and measurements

All commercially available chemicals were reagent grade and used as received. Elemental analyses of C, H and N were performed on a Perkin-Elmer 2400 elemental analyzer. IR spectra were recorded with a Spectrum one Fourier transform infrared (FT-IR) spectrometer using KBr pellets in the range of 400–4000 $cm^{-1}$. The power X-ray diffractions (PXRD) data of the samples was collected on a Rigaku D/MAX-3B diffractometer using Cu-K$\alpha$ radiation ($\lambda$ = 1.5418 Å) and 2$\theta$ ranging from 5 to 50°. Thermal analyses were conducted on a Perkin-Elmer STA 6000 with a heating rate of 10 °C $min^{-1}$ in a temperature range from 48 to 800 °C under air atmosphere. The circular dichroism spectra (CD) of **CCPs 1–4** were recorded at room temperature with a Jasco J-810(S) spectropolarimeter (KBr pellets). The luminescent spectrum was taken on a Perkin Elemer Corporation Model Fluorescence Spectrometer LS 55 PL. PL spectra were performed in solid samples after the crystals were solved in methanol. The second-order nonlinear optical intensities were estimated by measuring microcrystalline samples relative to urea by a Spectra Physics Quanta Ray Prolab 170 Nd:YAG laser using the first-harmonics output of 1064 nm with a pulse width of 10 ns and a repetition rate of 10 Hz.[7]

### Synthesis

**Synthesis of methyl 4′-((1-methoxy-1-oxopropan-2-yl)oxy)-[1,1′-biphenyl]-4-carboxylate (3a and 3b).** Methyl 4′-hydroxy-[1,1′-biphenyl]-4-carboxylate (**1**, 4.6 g, MW = 228.25, 0.020 mol), (*S*)-methyl lactate or (*R*)-methyl lactate (**2**, 2.2 g, MW = 104.11, 0.021 mol), triphenylphosphine (5.8 g, MW = 262.29, 0.022 mol) were mixed in dry 50 mL THF, to which diethyl diazocarboxylate (3.8 g, MW = 174.15, 0.022 mol) in 10 mL THF was dropwise added over 10 min at 0 °C. After stirring for 2 h at the same temperature, the reaction mixture was concentrated. Then, the residue was purified by flash column chromatography on silica gel eluting with 20% ethyl acetate in petroleum ether to give **3a** or **3b** (4.8 g, MW = 314.34, 0.015 mol, 76%) as a white solid.

**Synthesis of 4′-(1-carboxyethoxy)-[1,1′-biphenyl]-4-carboxylic acid (4a and 4b).** 4′-((1-Methoxy-1-oxopropan-2-yl)oxy)-[1,1′-biphenyl]-4-carboxylate (**3a** or **3b**, 6.3 g, MW = 314.34, 0.020 mol), 10 mL methanol, 40 mL water and solid sodium hydroxide (1.2 g, 0.030 mol) were added to a 100 mL round-bottomed flask containing a stirring bar. The reaction mixture was stirred and heated at 50 °C for 10 h, then the result solution was acidified to pH 1–2 with concentrated aqueous HCl in an ice bath. The precipitated solid was separated by filtration to give pure compound **4a** or **4b** (4.9 g, MW = 286.28, 0.017 mol, 85%) as a white solid. $^1$H NMR (400 MHz, DMSO-$d_6$), $\delta$ (ppm): 1.53 (d, $J$ = 6.78 Hz, 3H) 4.91 (q, $J$ = 6.69 Hz, 1H) 6.98 (d, $J$ = 8.78 Hz, 2H) 7.61–7.80 (m, 4H) 7.98 (d, $J$ = 8.28 Hz, 2H) 13.00 (br. s., 1H).

**Synthesis of methyl 6-((1-methoxy-1-oxopropan-2-yl)oxy)-2-naphthoate (6a and 6b).** To a solution of methyl 6-hydroxy-2-naphthoate (**5**, 4.0 g, MW = 202.21, 0.020 mol), (*S*)-methyl lactate or (*R*)-methyl lactate (**2**, 2.2 g, MW = 104.11, 0.021 mol) and triphenylphosphine (5.8 g, MW = 262.29, 0.022 mol) in dry 50 mL THF, diethyl diazocarboxylate (3.8 g, MW = 174.15, 0.022 mol) solution in 10 mL THF was dropwise added over 10 min at 0 °C. After stirring for 2 h at the same temperature, the reaction mixture was concentrated. Then, the residue was purified by flash column chromatography on silica gel-eluting with 20% ethyl acetate in petroleum ether to give **6a** or **6b** (4.3 g, MW = 288.30, 0.015 mol, 75%) as a white solid.

**Synthesis of 6-(1-carboxyethoxy)-2-naphthoic acid (7a and 7b).** Methyl 6-((1-methoxy-1-oxopropan-2-yl)oxy)-2-naphthoate (**6a** or **6b**, 5.8 g, MW = 288.30, 0.020 mol), 10 mL methanol, 40 mL water, and solid sodium hydroxide (1.2 g, 0.030 mol) were

added to a 100 mL round-bottomed flask containing a stirring bar. The reaction mixture was stirred and heated at 50 °C for 10 h, then the result solution was acidified to pH 1–2 with concentrated aqueous HCl in an ice bath. The precipitated solid was separated by filtration to give pure compound **7a** or **7b** (4.2 g, MW = 260.25, 0.016 mol, 80%) as a white solid: $^1$H NMR (400 MHz, DMSO-$d_6$), $\delta$ (ppm): 1.58 (d, $J$ = 6.78 Hz, 3H) 5.06 (q, $J$ = 6.69 Hz, 1H) 7.21–7.31 (m, 2H) 7.77–7.88 (m, 1H) 7.88–7.96 (m, 1H) 8.03 (d, $J$ = 8.78 Hz, 1H) 8.52 (s, 1H).

**Synthesis of [Zn((*R*)-cbca)]·$H_2O$] (CCP-1).** A mixture of (*R*)-$H_2$cbca (28.6 mg, 0.1 mmol), $Zn(NO_3)_2\cdot 6H_2O$ (29.7 mg, 0.1 mmol), 8 mL acetonitrile and distilled 2 mL water was stirred for 1 h in air and then transferred and sealed in a Teflon reactor (20 mL), which was heated at 120 °C for 3 days, then cooled to room temperature at a rate of 10 °C h$^{-1}$. Colorless crystals of **CCP-1** were obtained in 57% yield (based on $Zn(NO_3)_2\cdot 6H_2O$). Elemental analysis (%) calcd for **CCP-1** ($C_{16}H_{14}O_6Zn$) (367.64): C, 52.27; H, 3.84. Found: C, 52.11; H, 3.71. IR (KBr, cm$^{-1}$): 3269.5 (m), 1573.3 (s), 1528.1 (s), 1466.6 (s), 1424.2 (s), 1336.9 (m), 1245.7 (s), 1205.2 (m), 1085.6 (m), 1042.5 (m), 882.4 (w), 838.1 (m), 781.1 (m), 713.7 (w).

**Synthesis of [Zn((*S*)-cbca)·$H_2O$] (CCP-2).** The preparation of **CCP-2** was same as that of **CCP-1** except that (*S*)-$H_2$cbca (28.6 mg, 0.1 mmol) was used instead of (*R*)-$H_2$cbca. Colorless crystals of **CCP-2** were obtained in 53% yield (based on $Zn(NO_3)_2\cdot 6H_2O$). Elemental analysis (%) calcd for **CCP-2** ($C_{16}H_{14}O_6Zn$) (367.64): C, 52.27; H, 3.84. Found: C, 52.09; H, 3.69. IR (KBr, cm$^{-1}$): 3278.4 (m), 1581.6 (s), 1534.5 (s), 1473.6 (s), 1433.4 (s), 1343.2 (m), 1254.1 (s), 1210.4 (m), 1091.9 (m), 1051.5 (m), 890.5 (w), 846.4 (m), 789.1 (m), 722.3 (w).

**Synthesis of [Zn((*R*)-cna)·$2H_2O$] (CCP-3).** A mixture of (*R*)-$H_2$cna (26.0 mg, 0.1 mmol), $Zn(NO_3)_2\cdot 6H_2O$ (29.7 mg, 0.1 mmol), 8 mL acetonitrile and 2 mL distilled water was stirred for 1 h in air and then transferred and sealed in a teflon reactor (20 mL), which was heated at 140 °C for 3 days, then cooled to room temperature at a rate of 10 °C h$^{-1}$. Colorless crystals of **CCP-3** were obtained in 59% yield (based on $Zn(NO_3)_2\cdot 6H_2O$). Elemental analysis (%) calcd for **CCP-3** ($C_{14}H_{14}O_7Zn$) (359.62): C, 46.76; H, 3.92. Found: C, 46.51; H, 3.73. IR (KBr, cm$^{-1}$): 3386.2 (s), 3199.1 (s), 1558.5 (s), 1475.6 (s), 1408.1 (s), 1326.1 (m), 1215.2 (s), 1145.7 (m), 1103.3 (m), 1039.6 (m), 960.6 (w), 887.3 (m), 802.4 (w).

**Synthesis of [Zn((*S*)-cna)·$2H_2O$] (CCP-4).** The preparation of **CCP-4** was the same as that of **CCP-3** except that (*S*)-$H_2$cna (26.0 mg, 0.1 mmol) was used instead of (*R*)-$H_2$cna. Colorless crystals of **CCP-4** were obtained in 53% yield (based on $Zn(NO_3)_2\cdot 6H_2O$). Elemental analysis (%) calcd for **CCP-4** ($C_{14}H_{14}O_7Zn$) (359.62): C, 46.76; H, 3.92. Found: C, 46.64; H, 3.65. IR (KBr, cm$^{-1}$): 3373.4 (s), 3190.8 (s), 1549.4 (s), 1486.1 (s), 1400.9 (s), 1334.6 (m), 1205.7 (s), 1132.2 (m), 1114.6 (m), 1043.5 (m), 957.9 (w), 891.1 (m), 808.3 (w).

**X-ray crystallography.** Single-crystal X-ray diffraction data for **CCPs 1–4** were collected on a Rigaku R-AXIS RAPID imaging plate diffractometer with graphite-monochromated Mo Kα ($\lambda$ = 0.71073 Å) at 291 K. Empirical absorption corrections based on equivalent reflections were applied. The structures of **1–4** were solved by direct methods and refined by full-matrix least-squares methods on $F^2$ using SHELXS-97 crystallographic software package.[8] The crystal parameters, data collection and refinement results for **1–4** are summarized in Table 1. Selected bond lengths and angles of **1–4** are listed in Table S1† and the H-bond lengths and angles are shown in Table S2 (see the ESI†).

Table 1 Crystal data and structure refinement for **CCPs 1–4**[a,b]

| Crystal parameters | CCP-1 | CCP-2 | CCP-3 | CCP-4 |
|---|---|---|---|---|
| Empirical formula | $C_{16}H_{14}O_6Zn$ | $C_{16}H_{14}O_6Zn$ | $C_{14}H_{14}O_7Zn$ | $C_{14}H_{14}O_7Zn$ |
| Formula weight | 367.64 | 367.64 | 359.62 | 359.62 |
| Crystal system | Monoclinic | Monoclinic | Monoclinic | Monoclinic |
| Space group | $P2_1$ | $P2_1$ | $P2_1$ | $P2_1$ |
| $a$ (Å) | 5.7071(11) | 5.6961(11) | 6.0565(12) | 6.045(5) |
| $b$ (Å) | 7.8905(16) | 7.8959(16) | 7.3687(15) | 7.363(5) |
| $c$ (Å) | 15.868(3) | 15.870(3) | 15.825(3) | 15.846(5) |
| $\alpha$ (°) | 90 | 90 | 90 | 90 |
| $\beta$ (°) | 97.78(3) | 97.98(3) | 96.60 | 96.636(5) |
| $\gamma$ (°) | 90 | 90 | 90 | 90 |
| $V$ (Å$^3$) | 708.0(2) | 706.9(2) | 701.6(2) | 700.6(8) |
| $Z$ | 2 | 2 | 2 | 2 |
| $D_{caled}$ (Mg cm$^{-3}$) | 1.725 | 1.727 | 1.702 | 1.705 |
| $\mu$ (mm$^{-1}$) | 1.765 | 1.768 | 1.784 | 1.786 |
| Collected/unique | 6910/3103 | 5257/2414 | 6577/2802 | 2471/2464 |
| $R_{int}$ | 0.0423 | 0.0265 | 0.0242 | 0.0176 |
| GOF on $F^2$ | 1.107 | 1.076 | 1.088 | 1.079 |
| $R$ ($I > 2\sigma(I)$) | $R_1$ = 0.0354 | $R_1$ = 0.0274 | $R_1$ = 0.0254 | $R_1$ = 0.0428 |
| | w$R_2$ = 0.0915 | w$R_2$ = 0.0609 | w$R_2$ = 0.0567 | w$R_2$ = 0.1247 |
| $R$ (all data) | $R_1$ = 0.0419 | $R_1$ = 0.0302 | $R_1$ = 0.0274 | $R_1$ = 0.0445 |
| | w$R_2$ = 0.1064 | w$R_2$ = 0.0627 | w$R_2$ = 0.0575 | w$R_2$ = 0.1271 |

[a] $R_1 = (\sum||F_o| - |F_c|)/\sum|F_o|$. [b] $wR_2 = [\sum w(F_o^2 - F_c^2)^2/\sum w(F_o^2)^2]^{1/2}$.

 

## Results and discussion

### Crystal structure of [Zn((*R*)-cbca)·$H_2O$] (CCP-1) and [Zn((*S*)-cbca)·$H_2O$] (CCP-2)

The single-crystal X-ray crystallographic analysis reveals that **CCP-1** and **CCP-2** crystallized in monoclinic system with a chiral space group of $P2_1$. As shown in Fig. 1(a), the asymmetric unit consists of one Zn(II) ion, one (*R*)-cbca$^{2-}$ anion and one coordinated water molecule. The Zn(II) ion is five-coordinated by four carboxylate oxygen atoms from three different (*R*)-cbca$^{2-}$ anions and one coordinated water molecule. The geometry around the Zn(II) center can be described as a trigonal bipyramid. The Zn–O bond lengths are in the range of 1.963(3)–2.398(3) Å, the O–Zn–O bond angles vary from 58.44(11) to 138.45(12)°, which are all in the reasonable range. The two carboxylate groups of the ligand employ bidentate chelating and bridging coordination modes, respectively.

In **CCP-1**, an infinite right-handed helical chain along the *b*-axis is formed by a carboxylate group of the ligand bridging two Zn cations, comparatively, a homo left-handed helical chain is observed in **CCP-2**, the winding axis corresponds to the *b* axis and the pitch to the length of 7.896 Å. The adjacent chiral chains are further connected by the ligands to generate 2D wave-like layers (Fig. 2(b) and (c)). The 2D layers are further linked together by hydrogen bonds (O(6)–H(61)···O(4), O(6)–H(62)···O(2)) to eventually produce a 3D framework (Fig. 2(d)). The hydrogen bonding data are summarized in Table S1.† If the ligand is considered as a three-connected node, Zn(II) cation as a five-connected node and water molecule as a three-connected node, the framework of **CCP-1** can be simplified as a 3,5-connected hms 3,5-conn topological structure with a point symbol of $(6^3)(6^9\cdot 8)$ (Fig. 1(e)).

### Crystal structure of [Zn((*R*)-cna)·$2H_2O$] (CCP-3) and [Zn((*S*)-cna)·$2H_2O$] (CCP-4)

X-ray crystallographic analysis revealed that **CCP-3** and **CCP-4** crystallize in monoclinic system with chiral space group $P2_1$. The asymmetric unit in **CCP-3** contains one Zn(II) ion, one (*R*)-cna$^{2-}$ anion and two coordinated water molecules. Each Zn(II) ion in **CCP-3** was five-coordinated defined by two oxygen atoms from a carboxylate group and a alkoxyl group of one ligand, one oxygen atom from a carboxylate group of another ligand and two oxygen atoms from two coordinated water molecules. The Zn–O bond distances lie in the range of 1.9354(18)–2.4146(18) Å with the bond angles around each Zn(II) center ranging from 73.17(8) to 163.47(8)°, which are all in the normal range.

The outstanding structural feature of **CCP-3** and **CCP-4** is two types of 1D helical chains. Two Zn cations were connected by the (*R*)-cna$^{2-}$ anions to generate an infinite left-handed helical chain running along the *b*-axis in **CCP-3**, a comparative right-handed helical chain was formed in **CCP-4**, the winding axis corresponds to the *b* axis and the pitch to the length of 7.3687 Å (Fig. 2(b) and (c)). The 1D chiral helical chains are further linked together by hydrogen bonds (O(6)–H(61)···O(3), O(6)–H(62)···O(5), O(7)–H(71)···O(3), O(7)–H(72)···O(3)) to produce a three-dimensional (3D) framework (Fig. 2(d)). The hydrogen bonding data are summarized in Table S2.† From the view of topology, if the Zn(II) atom is considered as a 5-connected node, cna$^{2-}$ is viewed as a 5-connector, the structure of **CCP-3** can be simplified as a 5-connected network with a point symbol of $(4^4\cdot 6^6)$ (Fig. 2(e)).

The most obvious difference between the **CCPs** constructed by the two different ligands is the coordination modes of the ligands. In the two pairs of **CCPs** built by (*R*) and (*S*)-$H_2$cbca, (*R*) and (*S*)-$H_2$cna, the central Zn(II) atoms are all five-coordinated,

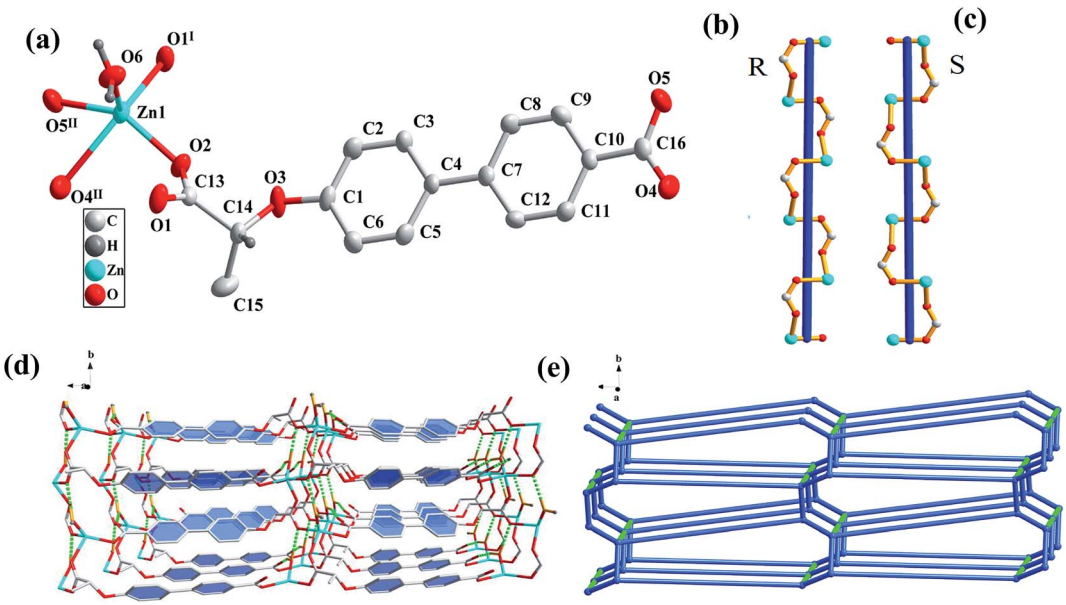


Fig. 1 (a) Stick-ellipsoid representation of the asymmetric unit of **CCP-1** (b) right-handed helical chain in **CCP-1** (c) left-handed helical chain in **CCP-2** (d) 2D grid network architecture made by an infinite right-handed helical chain running along *b*-axis. The layers linked together by hydrogen bonds to generate a 3D supramolecular architecture (e) schematic illustration of 3D 3,5-connected topological net with a point symbol of $(6^3)(6^9\cdot 8)$, symmetry codes: (I) $-x, y-1/2, -z+1$; (II): $x-1, y, z-1$.

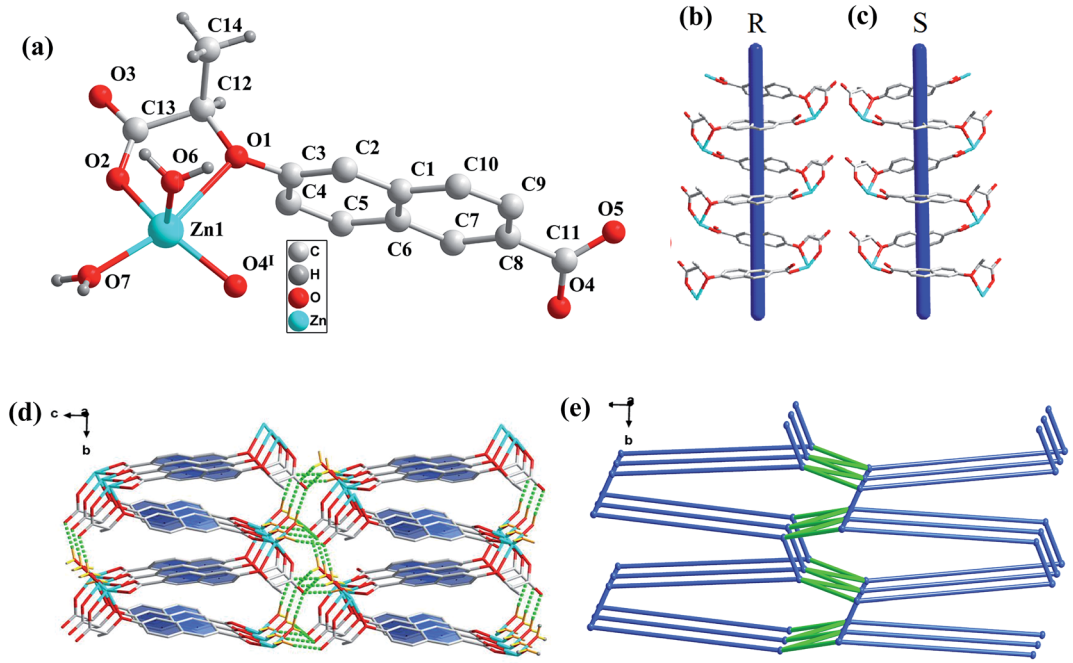


Fig. 2 (a) Stick-ellipsoid representation of the asymmetric unit of **CCP-3** (b) right-handed helical chain in **CCP-3** (c) left-handed helical chain in **CCP-4** (d) the right-handed helical chain generated by the connection of Zn(II) ion and the carboxylate group of the ligand and the three-dimensional supramolecular architecture constructed *via* hydrogen bonds interactions (e) schematic illustration of 3D 5-connected topological net with a point symbol of $(4^4 \cdot 6^6)$. Symmetry codes: (I) $-x, y - 1/2, -z + 1$.

however, different coordinating atoms of the ligands are involved. In **CCP-1** and **2**, for the ligands (*R*) or (*S*)-$H_2$cbca with biphenyl group, only the carboxylate oxygen atoms besides the coordinating water molecules are involved in the coordination, while in **CCP-3** and **4**, for the ligands (*R*) or (*S*)-$H_2$cna with naphthalene ring, an ether oxygen atom of the ligand also coordinates with Zn(II) atom. In **CCP-1** and **2**, the chiral carboxylate groups bridging coordinate with Zn(II) in μ2-η1:η1 and μ1-η1:η1 modes with a pitch to the length of 7.896 Å, while in **CCP-3** and **4** the chiral carboxylate groups chelating coordinate with Zn(II) by carboxylate group and ether group with a pitch to the length of 7.369 Å, which causes the helical repeating units changed from $\{$–Zn1–O2–C13–O3–$\}_n$ in **CCP-1** and **2** to $\{$–Zn1–(cna)2–$\}_n$ in **CCP-3** and **4**, leading to the eventual structural differences.

## Thermal analysis and PXRD results

The powder X-ray diffraction of **CCPs 1–4** were checked for the crystalline samples at room temperature. As shown in Fig. S5 and S6,† the peak positions of experimental and simulated PXRD patterns match well, which confirms their phase purity. The differences in intensity may be owed to the preferred orientation of the crystal samples.

To study the thermal stabilities of these **CCPs**, thermal gravimetric analysis (TGA) of **CCPs 1–4** was performed (Fig. S7–S10†). TGA curves have been obtained under an air atmosphere for crystalline samples in the temperature range 48–800 °C with a heating rate of 10 °C $min^{-1}$, showing that the two pairs of **CCPs** are all quite stable. **CCP-1** and **CCP-2** have two steps of weight loss. The first weight loss of 5.31% in the range of 50–235 °C is consistent with the removal of coordination water molecules (calcd, 4.89%). The second step of 235–595 °C can be attributed to the release of the ligand (found, 77.84%; calcd, 77.25%). Finally, the remaining weight is assigned to ZnO. Similarly, **CCP-3** and **CCP-4** also demonstrate two weight-loss processes. In **CCP-3** and **CCP-4**, the weight loss in the range of 48–210 °C corresponds to the removal of two coordination water molecules (found, 10.06%; calcd, 10.31%). At 300–545 °C, the weight loss can be attributed to the decomposition of the ligand. Finally, the remaining residue could be ascribed to the formation of ZnO (found, 22.11%; calcd, 22.52%).

## Circular dichroism spectra (CD) analysis

Considering that all the **CCPs** in this contribution crystallize in chiral space groups, their solid-state circular dichroism (CD) measurements have been performed to further demonstrate their homochirality (Fig. 3). As shown in Fig. 3(a), the CD spectrum for the bulk sample of **CCP-1** exhibit a positive Cotton effect with peaks at 332 nm and a negative Cotton effect at 250 nm. The CD spectrum for the bulk sample of **CCP-2** exhibits a negative Cotton effect with peak at 337 nm and a positive Cotton effect at 245 nm. The CD spectrum of **CCP-3** exhibits a positive Cotton effect with peak at 320 nm and a negative Cotton effect at 260 nm. Meanwhile, a mirror image is observed for **CCP-4** (as shown in Fig. 3(b)). In a word, the two pairs of **CCPs** have been confirmed to be enantiomers, respectively.

## Second harmonic generation (SHG) efficiency

As Verbiest pointed out, supramolecular aggregates and chirality could significantly enhance the nonlinear optical

 

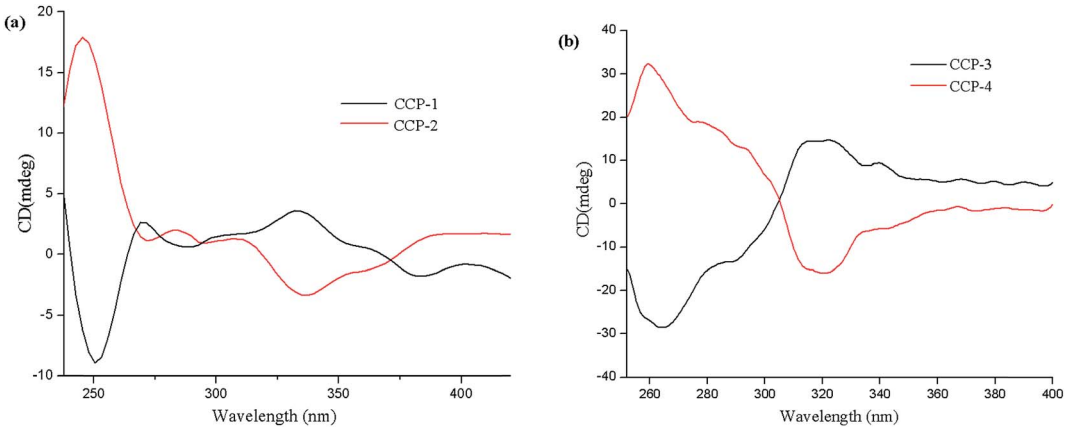


Fig. 3 (a) Solid-state CD spectra of **CCP-1** and **CCP-2** (b) solid-state CD spectra of **CCP-3** and **CCP-4**.

properties.[9] The nonlinear optical properties of Zn(II) based **CCPs 1–4** are investigated since they are crystallized in the noncentrosymmetric chiral space groups as the colorless crystals. In general, the second-harmonic generation (SHG) efficiency can be measured according to the method proposed by Kurtz and Perry by using a powder technique. The SHG efficiency of a standard material, such as α-quartz, $KH_2PO_4$ (KDP), or urea are compared with the sample. The efficiency of KDP is 16× α-quartz, whereas that of urea is 400× α-quartz. The technologically important $LiNbO_3$ is 600× α-quartz. In this work, the SHG efficiencies are compared with urea by using pure microcrystalline samples.

The preliminary experimental results indicated that the four **CCPs** have modest powder SHG efficiency up to 0.6, 0.6, 0.5, and 0.5 times, respectively, as much as that of urea. It was previously proposed that hydrogen bonding as a donor–acceptor system could significantly enhance the SHG response because hyperpolarizabilities strongly depend on the number molecules aggregated through H bonds.[10] Most reported **CCPs** possessing SHG efficiency are built by Zn anions as metal centers. Compared

Table 2 SHG activity comparison of Zn-based **CCPs** built from chiral ligands

| CCPs | Chemical formula | Dimension | Space group | SHG | Ref. |
|---|---|---|---|---|---|
| 1 | $[Zn((R)\text{-cbca})\cdot H_2O]$ | 3D | $P2_1$ | 0.6× urea | This paper |
| 2 | $[Zn((S)\text{-cbca})\cdot H_2O]$ | 3D | $P2_1$ | 0.6× urea | This paper |
| 3 | $[Zn((R)\text{-cna})\cdot 2H_2O]$ | 3D | $P2_1$ | 0.5× urea | This paper |
| 4 | $[Zn((S)\text{-cna})\cdot 2H_2O]$ | 3D | $P2_1$ | 0.5× urea | This paper |
| 5 | [Zn(cpfa)] | 3D | $P2_12_12_1$ | 0.3× urea | 12 |
| 7 | $[Zn(cpca)(H_2O)]_2\cdot(H_2O)$ | 2D | $C2$ | 0.5× urea | 13 |
| 8 | $Zn(SCMC)(H_2O)$ | 2D | $P2_1$ | 0.05× urea | 14 |
| 9 | $[Zn(bddp)\cdot(H_2O)_4]_2\cdot H_2O$ | 1D | $P2_1$ | 0.6× urea | 15 |

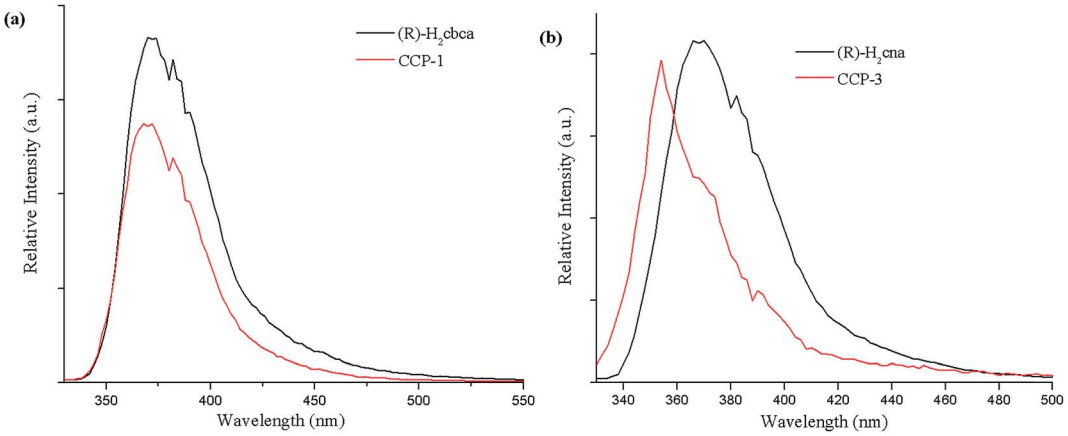


Fig. 4 (a) Solid state emission spectra of (*R*)-$H_2$cbca and **CCP-1** (excited at 350 nm) (b) solid state emission spectra of (*R*)-$H_2$cna and **CCP-3** (excited at 345 nm).

with several reported Zn-based **CCPs** built by chiral ligands, as listed in Table 2, **CCPs 1–4** show medium SHG activities. The SHG optical experimental result indicates that the four **CCPs** have the potential to be used as optical materials.[11]

### Luminescent studies

Luminescence properties of metal–organic **CCPs** have been widely investigated, owing to their potential applications in chemical sensors, photochemistry, and electroluminescent displays.[16] Therefore, in this work, the solid-state excitation (Fig. S13–S16†) and emission spectra for (*R*)-$H_2$cbca, (*R*)-$H_2$cna, **CCP-1** and **CCP-3** were studied in the solid state at room temperature (Fig. 4).

The main emission peaks of (*R*)-$H_2$cbca and (*R*)-$H_2$cna are at 372 nm ($\lambda_{ex}$ = 350 nm) and 368 nm ($\lambda_{ex}$ = 345 nm). The emission peak of the free ligand is probably attributable to the $\pi^* \rightarrow \pi$ or $\pi^* \rightarrow$ n transitions as reported. The emission spectra for **CCP-3** exhibit emission peak at 354 nm ($\lambda_{ex}$ = 345 nm). In comparison with (*R*)-$H_2$cna, the blue shift of emission maxima in **CCP-3** may be attributed to a charge transfer transition between ligand and metal center, Zn(II) ions with $d_{10}$ electron configuration are rather stable and are difficultly oxidized or reduced. Thus, compared to the emission peak of $H_2$cna ligand, the emissions of **CCP-3** may be assigned to intraligand (n–$\pi^*$ or $\pi$–$\pi^*$) emission. The similar emission energies between **CCP-1** and the free ligands indicate that their most possible luminescent mechanism originates from the ligand centered emission. For **CCPs 1–4** are highly thermally stable and insoluble in common solvents, they may be suitable as excellent candidates for the exploration of fluorescent materials.

## Conclusion

In summary, two pairs of enantiomers (*R*) and (*S*)-$H_2$cbca, (*R*) and (*S*)-$H_2$cna with slight structural differences have been employed to construct two pairs of homochiral coordination polymers with Zn(II). The most obvious difference between the two pairs of **CCPs** lies in the different coordinating atoms of the ligands. Compared with **CCP-1** and **2**, an ether oxygen atom of the ligand in **CCP-3** and **4** is also involved in the coordination besides the carboxylate oxygen atoms, leading to the differences of the pitch to the lengths of the helical repeating units. The SHG optical experimental results indicate that **CCPs 1–4** have medium SHG activities which could be used as potential optical materials. The luminescent studies show that their most possible luminescent mechanism originates from the ligand centered emission.

## Acknowledgements

This work is financially supported by the National Natural Science Foundation of China (no. 21371052 & 21272061), Scientific Research Fund of Heilongjiang Provincial Education Department (12531512).

## References

1 (*a*) D. N. Dybtsev, A. L. Nuzhdin, H. Chun, K. P. Bryliakov, E. P. Talsi, V. P. Fedin and K. Kim, *Angew. Chem., Int. Ed.*, 2006, **45**, 916–920; (*b*) J.-Z. Gu, Y.-H. Cui, J. Wu and A. M. Kirillov, *RSC Adv.*, 2015, **5**, 78889–78901; (*c*) S. R. Batten, N. R. Champness, X.-M. Chen, J. Garcia-Martinez, S. Kitagawa, L. Öhrström, M. O'Keeffe, M. P. Suh and J. Reedijk, *CrystEngComm*, 2012, **14**, 3001; (*d*) B. Chen, S. Xiang and G. Qian, *Acc. Chem. Res.*, 2010, **43**, 1115–1124; (*e*) Y. Cui, Y. Yue, G. Qian and B. Chen, *Chem. Rev.*, 2012, **112**, 1126–1162.

2 (*a*) Y. Liu, W. Xuan and Y. Cui, *Adv. Mater.*, 2010, **22**, 4112–4135; (*b*) Q. Zhu, T. Sheng, R. Fu, C. Tan, S. Hu and X. Wu, *Chem. Commun.*, 2010, **46**, 9001–9003; (*c*) W. J. Rieter, K. M. Pott, K. M. Taylor and W. Lin, *J. Am. Chem. Soc.*, 2008, **130**, 11584–11585; (*d*) D. Sun, Y. Ke, D. J. Collins, G. A. Lorigan and H.-C. Zhou, *Inorg. Chem.*, 2007, **46**, 2725–2734; (*e*) D. N. Dybtsev, M. P. Yutkin, E. V. Peresypkina, A. V. Virovets, C. Serre, G. Férey and V. P. Fedin, *Inorg. Chem.*, 2007, **46**, 6843–6845.

3 (*a*) E. V. Anokhina, Y. B. Go, Y. Lee, T. Vogt and A. J. Jacobson, *J. Am. Chem. Soc.*, 2006, **128**, 9957–9962; (*b*) W. Xuan, M. Zhang, Y. Liu, Z. Chen and Y. Cui, *J. Am. Chem. Soc.*, 2012, **134**, 6904–6907; (*c*) R. Vaidhyanathan, D. Bradshaw, J. N. Rebilly, J. P. Barrio, J. A. Gould, N. G. Berry and M. J. Rosseinsky, *Angew. Chem., Int. Ed.*, 2006, **45**, 6495–6499.

4 (*a*) L. Yu, X.-N. Hua, X.-J. Jiang, L. Qin, X.-Z. Yan, L.-H. Luo and L. Han, *Cryst. Growth Des.*, 2015, **15**, 687–694; (*b*) N. L. Strutt, H. Zhang and J. F. Stoddart, *Chem. Commun.*, 2014, **50**, 7455–7458; (*c*) X.-L. Yang and C.-D. Wu, *CrystEngComm*, 2014, **16**, 4907; (*d*) H.-Y. An, E.-B. Wang, D.-R. Xiao, Y.-G. Li, Z.-M. Su and L. Xu, *Angew. Chem.*, 2006, **118**, 918–922; (*e*) Z. X. Xu, Y. X. Tan, H. R. Fu, J. Liu and J. Zhang, *Inorg. Chem.*, 2014, **53**, 12199–12204.

5 (*a*) X. Xu, Y.-H. Yu, G.-F. Hou, X.-W. Li, C.-Y. Ren and D.-S. Ma, *Polyhedron*, 2016, **112**, 61–66; (*b*) Y.-H. Yu, C.-Y. Ren, G.-F. Hou, H. Ye and J.-S. Gao, *J. Coord. Chem.*, 2012, **65**, 4137–4146; (*c*) Y.-H. Yu, H.-T. Ye, G.-F. Hou, C.-Y. Ren, J.-S. Gao and P.-F. Yan, *Cryst. Growth Des.*, 2016, **16**, 5669–5677.

6 (*a*) Z.-X. Xu, Y. Xiao, Y. Kang, L. Zhang and J. Zhang, *Cryst. Growth Des.*, 2015, **15**, 4676–4686; (*b*) L.-H. Cao, Y.-L. Wei, Y. Yang, H. Xu, S.-Q. Zang, H.-W. Hou and T. C. W. Mak, *Cryst. Growth Des.*, 2014, **14**, 1827–1838; (*c*) Z.-X. Xu, L. Liu and J. Zhang, *New J. Chem.*, 2016, **40**, 1927–1929.

7 S. K. Kurtz and T. T. Perry, *J. Appl. Phys.*, 1968, **39**, 3798–3813.

8 G. M. Sheldrick, *Acta Crystallogr., Sect. A: Found. Crystallogr.*, 2008, **64**, 112–122.

9 T. Verbiest, *Science*, 1998, **282**, 913–915.

10 Y.-R. Xie, R.-G. Xiong, X. Xue, X.-T. Chen, Z. Xue and X.-Z. You, *Inorg. Chem.*, 2002, **41**, 3323–3326.

11 (*a*) N. Chen, M.-X. Li, P. Yang, X. He, M. Shao and S.-R. Zhu, *Cryst. Growth Des.*, 2013, **13**, 2650–2660; (*b*) C. Wang, T. Zhang and W. Lin, *Chem. Rev.*, 2012, **112**, 1084–1104; (*c*) X. Jing, C. He, D. Dong, L. Yang and C. Duan, *Angew.*

 

*Chem., Int. Ed.*, 2012, **51**, 10127–10131; (*d*) F. Song, C. Wang, J. M. Falkowski, L. Ma and W. Lin, *J. Am. Chem. Soc.*, 2010, **132**, 15390–15398; (*e*) Y. Q. Sun, J. C. Zhong, L. Ding and Y. P. Chen, *Dalton Trans.*, 2015, **44**, 11852–11859.

12 H.-T. Ye, C.-Y. Ren, G.-F. Hou, Y.-H. Yu, X. Xu, J.-S. Gao, P.-F. Yan and S.-W. Ng, *Cryst. Growth Des.*, 2014, **14**, 3309–3318.

13 L.-L. Liang, S.-B. Ren, J. Zhang, Y.-Z. Li, H.-B. Du and X.-Z. You, *Cryst. Growth Des.*, 2010, **10**, 1307–1311.

14 Y.-T. Wang, H.-H. Fan, H.-Z. Wang and X.-M. Chen, *J. Mol. Struct.*, 2005, **740**, 61–67.

15 H.-T. Zhang, Y.-Z. Li, T.-W. Wang, E. N. Nfor, H.-Q. Wang and X.-Z. You, *Eur. J. Inorg. Chem.*, 2006, **2006**, 3532–3536.

16 (*a*) M. Q. Wang, K. Li, J. T. Hou, M. Y. Wu, Z. Huang and X. Q. Yu, *J. Org. Chem.*, 2012, **77**, 8350–8354; (*b*) S. Li, J. Song, J. C. Ni, Z. N. Wang, X. Gao, Z. Shi, F. Y. Bai and Y. H. Xing, *RSC Adv.*, 2016, **6**, 36000–36010; (*c*) Y. Peng, A. J. Zhang, M. Dong and Y. W. Wang, *Chem. Commun.*, 2011, **47**, 4505–4507; (*d*) X.-L. Tang, X.-H. Peng, W. Dou, J. Mao, J.-R. Zheng, W.-W. Qin, W.-S. Liu, J. Chang and X.-J. Yao, *Org. Lett.*, 2008, **10**, 3653–3656; (*e*) X.-X. Wang, X.-Q. Wang, X.-Y. Niu and T.-P. Hu, *CrystEngComm*, 2016, **18**, 7471–7477.